

See discussions, stats, and author profiles for this publication at: <https://www.researchgate.net/publication/232227892>

# iTRAQ-Based Quantitative Protein Expression Profiling and MRM Verification of Markers in Type 2 Diabetes

ARTICLE in JOURNAL OF PROTEOME RESEARCH · OCTOBER 2012

Impact Factor: 4.25 · DOI: 10.1021/pr300798z · Source: PubMed

CITATIONS

18

READS

134

12 AUTHORS, INCLUDING:



**Prabhjit Kaur**

Georgetown University

19 PUBLICATIONS 179 CITATIONS

SEE PROFILE



**Nasser M Rizk**

Qatar University

37 PUBLICATIONS 330 CITATIONS

SEE PROFILE



**Tejaswita M Karve**

Georgetown University

8 PUBLICATIONS 80 CITATIONS

SEE PROFILE



**John Kwagyan**

Howard University

65 PUBLICATIONS 549 CITATIONS

SEE PROFILE

# iTRAQ-Based Quantitative Protein Expression Profiling and MRM Verification of Markers in Type 2 Diabetes

Prabhjit Kaur,<sup>†,||</sup> Nasser M. Rizk,<sup>‡,||</sup> Sereen Ibrahim,<sup>‡</sup> Noura Younes,<sup>§</sup> Arushi Uppal,<sup>†</sup> Kevin Dennis,<sup>†</sup> Tejaswita Karve,<sup>†</sup> Kenneth Blakeslee,<sup>‡</sup> John Kwagyan,<sup>||</sup> Mahmoud Zirie,<sup>§</sup> Habtom W. Resson,<sup>†</sup> and Amrita K. Cheema<sup>\*,†</sup>

<sup>†</sup>Department of Oncology, Lombardi Comprehensive Cancer Center at Georgetown University Medical Center, Washington D.C., United States

<sup>‡</sup>Department of Health Sciences, Qatar University, Doha, Qatar

<sup>§</sup>Hamad Medical Corporation, Doha, Qatar

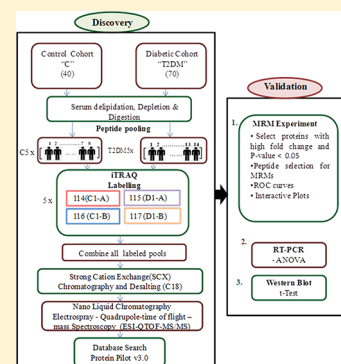
<sup>‡</sup>Waters Corporation, Washington, D. C., United States

<sup>||</sup>Howard University College of Medicine, Washington, D. C., United States

## Supporting Information

**ABSTRACT:** The pathogenesis of Type 2 diabetes mellitus (T2DM) is complex owing to molecular heterogeneity in the afflicted population. Current diagnostic methods rely on blood glucose measurements, which are noninformative with respect to progression of the disease to other associated pathologies. Thus, predicting the risk and development of T2DM-related complications, such as cardiovascular disease, remains a major challenge. We have used a combination of quantitative methods for characterization of circulating serum biomarkers of T2DM using a cohort of nondiabetic control subjects ( $n = 76$ ) and patients diagnosed with T2DM ( $n = 106$ ). In this case-control study, the samples were randomly divided as training and validation data sets. In the first step, iTRAQ (isobaric tagging for relative and absolute quantification) based protein expression profiling was performed for identification of proteins displaying a significant differential expression in the two study groups. Five of these protein markers were selected for validation using multiple reaction-monitoring mass spectrometry (MRM-MS) and further confirmed with Western blot and QPCR analysis. Functional pathway analysis identified perturbations in lipid and small molecule metabolism as well as pathways that lead to disruption of glucose homeostasis and blood coagulation. These putative biomarkers may be clinically useful for subset stratification of T2DM patients as well as for the development of novel therapeutics targeting the specific pathology.

**KEYWORDS:** Diabetes, Proteomics, Biomarkers, MRM, metabolic syndrome



## INTRODUCTION

Type 2 diabetes mellitus (T2DM) is a multifactorial metabolic disorder that is characterized by hyperglycemia and a number of comorbidities including cardiovascular disease (CVD), obesity, and metabolic syndrome.<sup>1–3</sup> The altered expression of genes and gene products in T2DM leads to the disruption of glucose homeostasis, which impacts multiple organs and poses dire threats to public health.<sup>4</sup> Methods measuring elevated blood glucose levels are not informative about the complex pathology, risk, and extent of progression and organ damage in T2DM. In addition, lack of sensitivity of these methods results in late disease diagnosis and poor prognosis. Thus, a multivariable panel of biomarkers is likely to have more predictive value than a single marker for T2DM.<sup>3,5,6</sup> Mass spectrometry-based quantitative biomarker profiling and verification approach is a powerful tool used to understand the global molecular interconnections that define the pathogenesis of T2DM. This information can also be used to gain mechanistic insights into disruption of signaling pathways and

networks that can be targeted for development of therapeutics for T2DM.

In recent times, several published studies have used a proteomic approach for global characterization of altered proteins in T2DM<sup>7,8</sup> or associated comorbidities, such as CVD,<sup>9</sup> diabetic neuropathy,<sup>10–12</sup> and retinopathy.<sup>13–16</sup> During the past decade, the effect of elevated glucose on protein level alterations in islet cells<sup>17–19</sup> as well as in serum<sup>20–23</sup> has been demonstrated using MALDI-TOF, SELDI-TOF, and LC-MS/MS analysis. However, there is a paucity of clinical studies reporting biomarker discovery and validation in T2DM as well as the elucidation of interactive networks that would fully exploit the power of the quantitative proteomics approach.

We hypothesize that the levels of circulating proteins in the serum of patients diagnosed with T2DM would be altered as compared with that of the control cohort. To elucidate

Received: August 23, 2012

Published: October 10, 2012

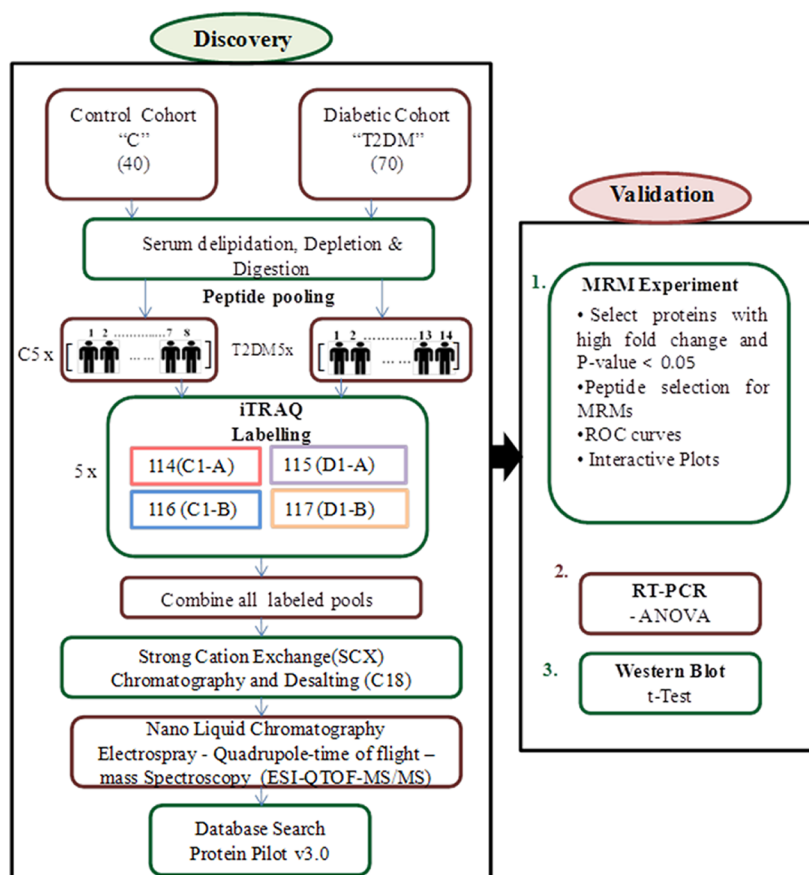


**Figure 1.** Overall workflow for discovery (iTRAQ) and verification (MRM) experiments. Serum samples were obtained from 40 healthy volunteers and 70 patients diagnosed with Type 2 diabetes mellitus (T2DM) under 12 h fasting conditions. Samples were randomly pooled to generate five biological pools for iTRAQ-based molecular profiling. Subsequently, five proteins with significantly high fold change were selected for MRM-based biomarker verification using an independent cohort of 72 control/T2DM samples. Some of the proteins were also validated by RT-PCR and Western blotting.

differentially expressed proteins in T2DM, we used a combination of untargeted and targeted quantitative proteomic approach in a clinical cohort. In the first step, global protein expression profiling using the iTRAQ (isobaric tagging for relative and absolute quantification) in serum samples obtained from controls ( $n = 40$ ) and patients diagnosed with T2DM ( $n = 70$ ) is performed. On the basis of this proteome map, peptides uniquely identifying the target proteins are selected; Q1/Q3 transitions are identified, and MRM (multiple reaction monitoring) methods are validated using the MarkerLynx "Intellistart" tool. The target proteins are quantified in an independent cohort of controls ( $n = 36$ ) and T2DM patients ( $n = 36$ ) by MRM. This approach enables us to reliably quantify the protein levels in the two study groups. Altered expression is further confirmed by Western blot and Q-PCR analysis. Finally, functional pathway analysis reveals significant alterations in diverse molecular networks and biological pathways across healthy and T2DM groups. The overall workflow is presented in Figure 1.

## MATERIALS AND METHODS

### Reagents

All the chemicals and solvents were of analytical grade or LC-MS grade. Acetonitrile (ACN) and water were obtained from Fisher Scientific (New Jersey, U.S.A.). Methyl methanethiosulfonate (MMTS) and Tris 2-carboxyethylphosphine (TCEP)

were purchased from Thermo Scientific (Rockford, U.S.A.). Diisopropyl ether and butanol were purchased from ACROS (New Jersey, USA).

### Serum Samples

Healthy human volunteers and patients diagnosed with T2DM were recruited at the Hamad medical hospital for blood collection in accordance with approved Institutional Review Board (IRB) protocols. We performed a case-control study involving a total of 182 subjects, who were randomly divided as training and verification data sets. All participants signed informed consent forms and responded to a detailed questionnaire capturing demographic and familial history of T2DM. Subsequent to 12 h of fasting, blood samples were collected from healthy volunteers and diabetic patients. Serum, plasma, and buffy coat were separated from whole blood and stored at  $-80^{\circ}\text{C}$  within 4 h of collection and aliquoted extensively to avoid repeat freeze thaw cycles. The serum glucose and high-density lipoprotein cholesterol (HDL-C) were assayed by automated clinical laboratory methods using a diagnostic analyzer (Roche, Mannheim, Germany). Low-density lipoprotein cholesterol (LDL-C) level was estimated using the Friedewald formula;  $\text{LDL-C} = \text{TC} - \text{HDL-C} - (\text{TG}/5)$ .<sup>24</sup>

### Serum Preparation for iTRAQ Analysis

**Delipidation of Serum Samples.** Since lipids interfere with iTRAQ labeling as well as detection of peptides by mass

spectrometry, the serum samples were delipidated according to the protocol described by Cham and Knowles.<sup>25</sup> Briefly, 3  $\mu$ L of 0.01 M EDTA was added to 100  $\mu$ L of serum, vortexed and placed on ice for 5 min, followed by addition of 200  $\mu$ L of delipidation buffer (di-isopropyl ether/butanol [60:40]) and mixed on a rotor (Labquake, Thermo Scientific) for 30 min at 4 °C. The tubes were centrifuged at 800g for 2 min at 4 °C. The serum layer was aspirated and transferred into a fresh microfuge tube without disturbing the lipid layer. The samples were dried under vacuum.

**High-Abundance Protein Depletion.** To enhance the detection and identification of medium- and low-abundance proteins, different immuno-depletion methods have been used.<sup>26</sup> In this study, the ProteoExtract Albumin/IgG Kit from Calbiochem (Merck Chemicals, USA) and Vivapure anti-HSA/IgG Kit (Sartorius, Germany) were used to evaluate the efficiency of high-abundance protein depletion from serum samples (Supporting Information Figure S1) using the instructions from the manufacturer. The total protein concentration was calculated by Bradford assay.<sup>27</sup> The Vivapure anti-HSA/IgG Kit was used for the iTRAQ experiment.

**Sample Pooling.** Multiple measurements using iTRAQ are cost-prohibitive, and hence, sample pooling has been used in proteomics experiments, which serves to reduce overall variability by minimizing individual heterogeneity.<sup>28,29</sup> We used a two-pronged strategy to determine the optimal method to conduct proteomic expression profiling studies with control and T2DM serum samples (Supporting Information Figure S2). Equal amounts of 10 serum samples each from the control (C) and T2DM (D) groups were delipidated and immuno-depleted, as described previously.

**Pooling Strategy A.** Serum samples from each group were combined to generate two sample pools, and 100  $\mu$ g of total protein from each pool was used for trypsin digestion and labeled with iTRAQ 114 (C1) and 115 (D1), respectively, and combined.

**Pooling Strategy B.** Ten serum samples each from T2DM and control cohort (total 20) were delipidated and immuno-depleted separately. Trypsin digestion was performed with 10  $\mu$ g of protein from each sample. At this stage, the peptides from each individual sample digest were pooled for each group, thus generating two sets of peptide pools (control and T2DM). The trypsin ratio was kept constant in both cases by adjusting the concentration such that 10  $\mu$ g of trypsin was used per 100  $\mu$ g of total protein in both cases. The pooled peptide mixtures were labeled with iTRAQ 116 (C2) and 117 (D2), respectively. The iTRAQ-labeled samples were fractionated using strong cation exchange chromatography and desalted for nano-LC-MS/MS analysis for both sample types. The underlying idea was to see if pooling of trypsin-digested serum samples would yield better results than pooling the serum samples at the first step.

### iTRAQ Labeling

For serum samples from the control cohort, an equal amount of total protein (12.5  $\mu$ g) per sample was trypsin-digested. Subsequently, the 40 control samples were divided into five pools by randomly pooling eight trypsin-digested samples for each pool. Similarly, five pools for the diabetic cohort were generated by random pooling 14 trypsin-digested peptide samples in each pool. Protein denaturation, digestion, and iTRAQ labeling were performed per the instructions of the manufacturer (iTRAQ 4-plex kit, ABSCIEX, USA). Briefly, protein pellets for individual samples were dissolved in 20  $\mu$ L of

dissolution buffer (ABSCIEX, USA), followed by addition of 1  $\mu$ L of SDS (2%) to each vial. This was followed by the addition of 2  $\mu$ L of reducing agent (50 mM TCEP). The samples were incubated at 60 °C for 1 h, 1  $\mu$ L of MMTS (200 mM) was added as a cysteine-blocking agent, and the samples were incubated for an additional 10 min at room temperature. Serum samples were digested with trypsin (ABSCIEX, USA), reduced with 10 mM dithiothreitol, and alkylated with 20 mM iodoacetamide. The peptides were labeled with iTRAQ reagents per the manufacturer's protocol and quenched with Milli-Q water. Sample labeling was as follows: Control serum (C1-A and C1-B) with iTRAQ reagents 114 and 116, and T2DM serum (D1-A and D1-B) with 115 and 117 tags, respectively, so as to run the same sample in duplicate in each run. Five such biological pools were generated by randomly pooling  $n = 10$  for the control group and  $n = 14$  for the T2DM cohort (Figure 1).

### Resolution with Strong Cation Exchange Chromatography (SCX)

The labeled samples were mixed and fractionated via strong cation exchange chromatography with Macrospin SCX columns (Nest Group, Inc., Southborough, MA). Fractions were eluted using stepwise salt plugs of 12 different molar concentrations of 100–800 mM sodium chloride. Each fraction was desalted using reverse-phase C18 spin columns (Nest Group, Inc. USA), as per the manufacturer's protocol, evaporated to dryness under vacuum, and stored at –80 °C until nano-UPLC-MS/MS analysis.

### Nano-UPLC-MS/MS Analysis

Nano UPLC-MS/MS analysis was conducted by an electrospray quadrupole time-of-flight (ESI-QTOF) mass spectrometer (QSTAR Elite, ABSCIEX, USA) coupled with a Nano-Acquity-UPLC system. The mobile phases consisted of solvent A (98% water, 2% acetonitrile, and 0.1% formic acid) and solvent B (98% ACN, 2% water, and 0.1% formic acid). The SCX fractionated and desalted peptides were dissolved in 2% ACN and 0.1% HCOOH and loaded on a nano-Acquity-UPLC Symmetry C18 trap column (180  $\mu$ m  $\times$  20 mm  $\times$  5  $\mu$ m). The column and the autosampler were maintained at a temperature of 40 and 4 °C, respectively. Chromatographic separation was performed using a BEH C18 column (75  $\mu$ m  $\times$  150 mm  $\times$  1.7  $\mu$ m). The nano-UPLC gradient delivered at 300 nL/min and consisted of a linear gradient of mobile phase B initiating from solvent B, 5–40% over 150 min. The mass spectrometer was operated in positive ion mode with a resolution of 10 000–12 000 at full width half-maximum for the QSTAR Elite using a source temperature of 200 °C. Altogether, 12 runs (fractions) were performed to finish one experiment. For MS/MS analysis, survey scans were acquired from  $m/z$  300 to 1500 with up to two precursors selected for MS/MS from  $m/z$  100 to 2000 using dynamic exclusion, and the rolling collision energy was used to promote fragmentation. To gain statistical evidence for differential expression of proteins, five separate experiments were performed as described above.

### iTRAQ Data Analysis

Relative abundance quantitation, peptide, and protein identifications were performed using Protein Pilot software 3.0 (ABSCIEX). Data were analyzed with MMTS as a fixed modification of cysteine, and the database was searched with a confidence interval of 95%, controlling for a 5% false discovery rate for protein identifications. Each MS/MS spectrum was



searched for species of *Homo sapiens* against the Uniprot database, which has 23 994 583 sequence entries.<sup>30</sup> The searches were run using the following parameters: fixed modification of methyl-methane-thiosulfate-labeled cysteine; fixed iTRAQ modification of free amine in the amino terminus and lysine; variable iTRAQ modifications of tyrosine; and allowing serine and threonine residues to undergo a side reaction with the iTRAQ reagent. Relative quantification of proteins in the case of iTRAQ was performed on the MS/MS scans and the ratio of the areas under the peaks at 114.1, 115.1, 116.1, and 117.1 *m/z*, corresponding to the mass-to-charge ratio of the iTRAQ reagents. The relative amounts of a peptide in each sample were calculated by dividing the peak areas observed at 115.1 and 117.1 *m/z* by that observed at 114.1 and 116.1 *m/z*. The following criteria were required to consider a protein for further statistical analysis: two or more high confidence (95%) unique peptides had to be identified, the *p* value in the protein quantitation had to be  $p \leq 0.05$ , and the fold difference had to be greater than 1.5. The peptides without any modification of free amine in the amino terminus or without iTRAQ modification of free amine in the lysine were excluded from calculation of the protein ratios.

#### Peptide Selection and Optimization of Multiple Reaction Monitoring (MRM) Method/Assay

High-confidence peptides of the target proteins exhibiting rich product ion spectrum were selected for MRMs (Supporting Information Figure S4A–J). The MRM analyses were performed on a triple quadrupole mass spectrometer (Xevo TQ-S, Waters Corporation, USA) interfaced with the nano-Acquity UPLC system. Test runs with the standard peptides were performed for transition selection and MRM method optimization using the “Intellistart” feature of the Xevo TQ-S. Two transitions, mainly *y* ions, were chosen for each peptide, two peptides were analyzed for each target protein, and all MRM analyses were run in triplicate. The amount of internal standard was optimized to get an optimal peak area ratio for normalization and relative quantitation. The peptide digest was separated on a Waters nano-Acquity UPLC system configured with a 5  $\mu\text{m}$  symmetry C18 trapping column (180  $\mu\text{m} \times 20\text{ mm}$ ) and a BEH130 C18 analytical column (75  $\mu\text{m} \times 150\text{ mm}$ , 1.7  $\mu\text{m}$ ). Five microliters of sample was injected and loaded onto the trapping column with a mobile phase composition of 99% A (0.1% formic acid in deionized water) and 1% B (0.1% formic acid in acetonitrile) at a flow rate of 300 nL/min. The source temperature was set to 70 °C, and the capillary voltage was set to 3.34 kV. The purge and cone gas flows were set to 0 and 35 mL/h, respectively. The nebulizer and nanoflow pressure were set to 7.0 and 0.25 bar, respectively. The collision gas (argon) flow was set to 0.15 mL/min. Resolutions for quadrupole 1 and quadrupole 2 were set to 1 and 0.75 Da, respectively. Following the trapping step, the flow rate was set to 300 nL/min, and the sample was flushed onto the analytical column. The column was held at 50 °C. The initial mobile phase condition of 1% B was held for 10 min. The percent of B was increased to 50% over 30 min, followed by an increase to 90% B in 5 min. The mobile phase was held at 90% B for 5 min and then at 1% B for 16 min to re-equilibrate the column. The total running time was 66 min.

#### Statistical Analysis of MRM data

MRM data were processed using TargetLynx 2.0. The relative quantification values of peptides were determined by calculating the ratio of peak areas of transitions of target peptides in

T2DM and control samples normalized to the peak area of the internal standard. The Graph pad Prism program v 5.0 was used for statistical analysis and to generate the receiver operating characteristic (ROC) curves and the interactive distribution plots. The Wilcoxon test, a nonparametric test, was used for the comparison of each peptide. Cutoff for significance was set at  $p \leq 0.05$ .

#### Western Blot

Immuno-depleted serum extracts containing 50  $\mu\text{g}$  of total protein from control and T2DM subjects were resolved by 1D gel electrophoresis on 4–20% bis-tris NuPAGE gradient gels (Invitrogen), transferred onto polyvinylidene fluoride membranes (Millipore Corporation, Bedford, MA) and blotted using six different primary antibodies: anti-apolipoprotein A 1 (mouse monoclonal, 1:1000 dilution); antitransferrin (mouse monoclonal, 1:2000); anti-vitamin D-binding protein (mouse monoclonal, 1:2000); anti-gelsolin (rabbit monoclonal, 1:1000); anti-ceruloplasmin (rabbit monoclonal, 1:1000); anti-angiotensin (rabbit monoclonal, 1:1000); and  $\beta$ -actin (rabbit polyclonal, 1:1000). The membranes were then incubated with the appropriate goat anti-mouse (Millipore, 1:1000); and goat anti-rabbit (Millipore, 1:1000) secondary antibodies, and the resultant complexes were detected using the enhanced chemiluminescence detection system (Santa Cruz). Detection was performed with autoradiography films (BioMax Light Film, Eastman Kodak, Rochester, NY). Densitometry analysis was performed using Image-J software, and protein-to- $\beta$ -actin ratios were expressed as means  $\pm$  SD from three independent experiments. *P*-values were calculated using the *t* test.

#### Quantitative Real-Time PCR (Q-PCR) Analysis

Total RNA was extracted from serum samples using the miRNeasy Mini Kit (Qiagen, Valencia, CA) as per the manufacturer's instructions. The extracted RNA was treated with DNase in the RNase-Free DNase Set (Qiagen) for 25 min to eliminate any contaminating DNA. Aliquots of clean RNA (70 ng) were used to synthesis first-strand cDNA strand by utilizing iScript Reverse Transcriptase Kit (Biorad, Hercules, CA) as per the manufacturer's instructions. Q-PCR was performed by the ABI PRISM 7900HT Sequence Detection System (Applied Biosystems, Foster City, CA). Each 25  $\mu\text{L}$  reaction consisted of appropriate gene-specific primers, cDNA template, and RT2 SYBR Green ROX QPCR Mastermix (Qiagen). Q-PCR primers for vitamin D-binding protein (GC) and beta actin ( $\beta$ -actin) were obtained from Real Time Primers, LLC (Elkin Parks, PA), and transthyretin (TTR) primers were purchased from Qiagen. The primer sequences when available as well as reaction conditions and expected product size are shown in Supporting Information Table ST1. Cycle threshold values for each reaction were adjusted automatically, and the fold changes for each pair of gene-specific primers were determined. The fold-change values were derived relative to the control and are represented as means  $\pm$  SEMs of mRNA expression normalized to  $\beta$ -actin, and a comparison was made using ANOVA.

## RESULTS

#### Experimental Strategy

In this study, we investigated the baseline changes in the serum proteome of patients diagnosed with T2DM as compared with those from a nondiabetic cohort under 12 h fasting conditions.

Biochemical analysis of serum showed an elevation in serum glucose, HbA<sub>1c</sub>, and insulin levels<sup>31</sup> and a decrease in the levels of vitamin D and HDL in the diabetic cohort (Table 1).

**Table 1. Characteristics of T2DM ( $n = 106$ ) and non-diabetic control ( $n = 76$ ) volunteers<sup>a</sup>**

	control	T2DM
clinical characteristics	32.2 ± 1.45	53.6 ± 1.43
age	28.9 ± 0.97	32.37 ± 0.97
BMI(kg/m <sup>2</sup> )	5.57 ± 0.05	7.66 ± 0.06
HbA <sub>1c</sub> (%)	17.5 ± 1.40	12.90* ± 1.34
vitamin D (ng/mL)	4.88 ± 0.05	8.71** ± 0.10
glucose (mM)	1.16 ± 0.77	1.72 ± 0.90
LDL (mM)	2.80 ± 0.05	2.54 ± 0.07
HDL (mM)	4.00 ± 1.23	1.23** ± 0.01
insulin (pM)	72.2 ± 3.69	91.43* ± 4.52

<sup>a</sup>The value spreads within the group for each parameter are indicated as mean ± standard error. The clinical parameters that had a significant change ( $P \leq 0.05$ ) between the control and T2DM groups are indicated with an asterisk.

Traditionally, glucose elevation has been used for diagnosis and clinical management of T2DM; however, serum glucose levels are not informative about the pathogenesis of T2DM, and hence, it is critical to understand the overall molecular changes that accompany the progression of T2DM, possibly leading to a myriad of physiological complications, including cardiovascular disease, blindness, and kidney and liver damage. The overall strategy is outlined in Figure 1. A total of 182 nondiabetic control and T2DM subjects were randomly divided as training and validation sets in this case-control study.

The characteristics of the study population are described in Table 1. For the discovery phase experiments, control ( $n = 40$ ) and T2DM ( $n = 70$ ) serum samples were pooled within the group to generate five pools to minimize individual variability (Figure 1). To maximize protein identification from immuno-depleted serum samples, we tested two different pooling strategies for iTRAQ analyses (Supporting Information Figures S2 and S3). Consistent with earlier reports,<sup>32</sup> we found a significant increase in the number of detected proteins as well as associated peptides when the samples were pooled after trypsin digestion and, hence, used this technique for the

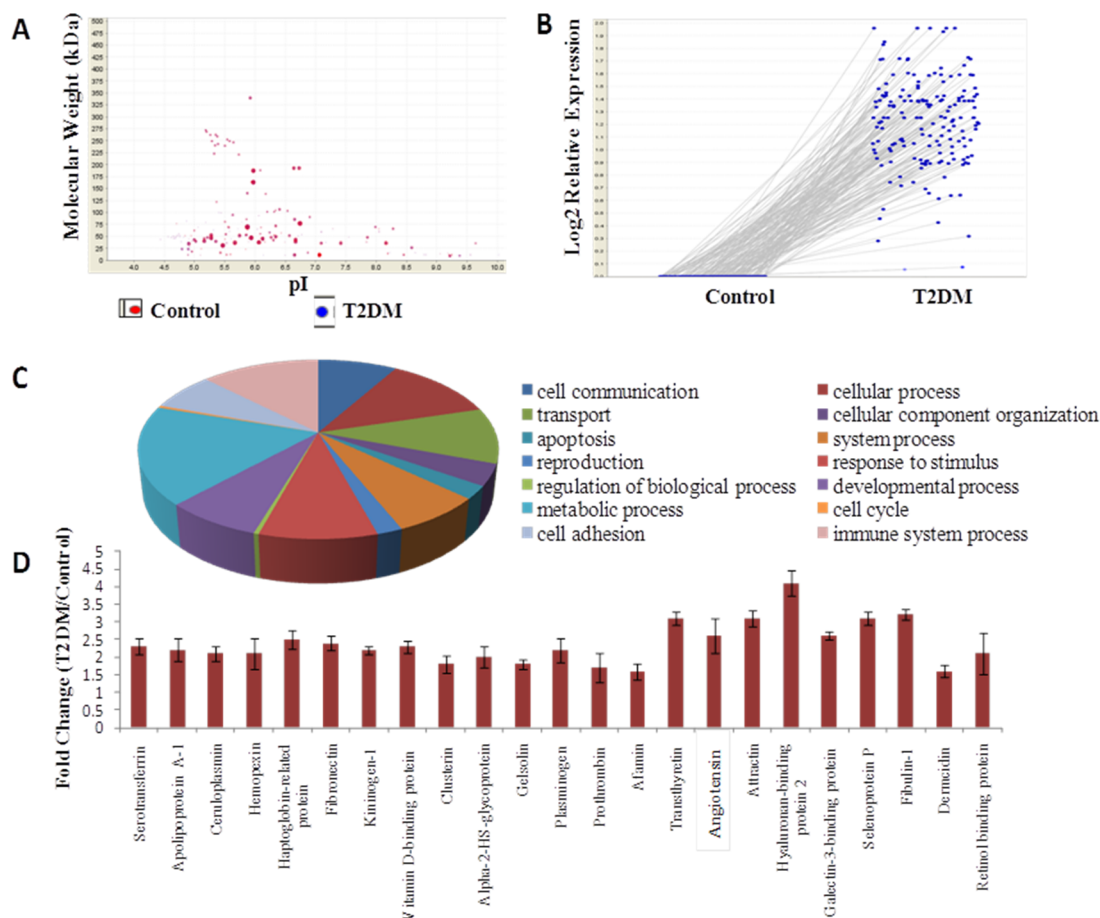


**Figure 2.** iTRAQ-based protein expression profiling facilitates biomarker discovery in Type 2 diabetes mellitus (T2DM). (Panel A) A 2D gel view of proteins detected by iTRAQ analysis showed comprehensive proteome coverage in the physiological pH range as well as a broad molecular weight range. Spot size reflects protein abundance based on spectral counts. The proteins in the control samples are represented in red and the T2DM in blue; magenta spots indicate the presence of the protein in both the groups. The superimposed data points represent the reproducibility of results across the five biological iTRAQ-labeled pools analyzed in duplicate. (Panel B) Pairwise comparison of protein intensities in the two study groups using the control sample as a baseline shows differential expression of proteins in the two study groups. (Panel C) Gene ontology analysis of the differentially expressed proteins in T2DM using PANTHER (Protein Analysis through Evolutionary Relationships), which uses the gene ontology for classifications by molecular function, biological process, and cellular components. (Panel D) Plot of select panel of proteins showing significant differential expression in the control and T2DM groups with  $p$  value  $\leq 0.05$ .

Table 2. Differentially Expressed Proteins Identified by iTRAQ Analysis<sup>a</sup>

accession no.	protein name	FC (T2DM/Q	p value	peptides CI (95%)	% coverage	MS/MS expt <sup>b</sup>
P02787	serotransferrin	↑	0.01	158	90	10
Q08380	galectin- 3 -binding protein	↑	0.02	12	21	6
P49908	selenoprotein P	↑	0.01	10	17	6
P00738	haptoglobin beta chain	↑	0.05	25	60	5
P22352	glutathione peroxidase 3	↑	0.04	9	9	6
P01009	α-1-antitrypsin	↑	0.01	58	99	10
P00450	ceruloplasmin	↑	0.01	47	60	10
P03952	plasma kallikrein light chain	↑	0.05	9	30	7
P02749	apolipoprotein H	↑	0.04	11	15	6
P04114	apolipoproteinB-100	↑	0.05	15	14	6
P05090	apolipoprotein D	↑	0.04	17	30	8
P02647	apolipoproteinA-1	↑	0.02	10	32	9
O14791	apolipoprotein LI	↑	0.02	10	26	7
P06727	apolipoprotein A-IV	↑	0.05	18	50	8
P02656	apolipoprotein C–III	↑	0.04	23	23	7
P02652	apolipoprotein A-II	↑	0.02	30	31	8
P02649	apolipoprotein E	↑	0.02	26	59	5
P05543	thyroxine-binding globulin	↑	0.02	12	14	9
P02765	α-2-HS-glycoprotein	↑	0.03	14	22	6
P08697	α-2-antiplasmin	↑	0.04	20	30	5
P08185	corticosteroid-binding globulin	↑	0.05	12	10	5
Q99727	metalloproteinase inhibitor4	↑	0.05	14	29	4
P05546	heparin cofactor 2	↑	0.05	15	28	4
P29622	kallistatin	↑	0.04	15	15	8
P01019	angiotensin	↑	0.01	12	17	10
P01023	α-macroglobulin	↑	0.03	25	9	7
P23142	fibulin	↑	0.04	12	11	9
P02655	apolipoprotein C–II	↑	0.03	13	20	7
P27708	Dihydroorotase	↑	0.03	14	22	6
O00625	pirin	↑	0.04	20	35	6
Q14520	hyaluronan-binding protein	↑	0.02	11	15	10
Q7Z5P9	mucin	↑	0.02	9	12	7
P02751	fibronectin	↑	0.01	6	14	10
P51884	lumican	↑	0.04	12	5	6
P22792	carboxypeptidase N subunit 2	↑	0.04	20	4	8
P02750	leucine-rich alpha-2-glycoprotein	↑	0.05	22	6	8
P04217	α-1B-ly coprote in	↑	0.03	7	50	7
Q9NVD7	parvin	↑	0.05	3	44	7
Q13835	plakophilin	↑	0.05	2	14	8
P20700	lamin	↓	0.04	2	11	8
P06396	gelsolin	↑	0.02	16	66	7
P43251	biotinidase	↑	0.05	1	19	5
P12270	nucleoprotein TPR	↑	0.05	1	11	6
043866	CD5 antigen-like	↑	0.04	0	19	8
P00747	plasminogen	↑	0.02	2	18	7
Q92954	proteoglycan 4	↑	0.03	2	28	7
O75636	ficolin	↑	0.03	3	11	6
P50895	Lutheran blood group glycoprotein	↑	0.03	2	9	7
Q92954	proteoglycan 4	↑	0.03	0	58	6
Q12955	reversed ankyrin-3	↑	0.05	5	30	7
P17661	desmin	↑	0.05	5	37	7
P03952	plasma kallikrein	↑	0.05	4	31	7
P04196	histidine-rich glycoprotein	↑	0.04	12	22	7
P04070	vitamin K-dependent protein C	↑	0.04	15	14	8
P07996	thrombospondin-1	↑	0.01	10	11	8
P27169	serum paraoxonase/arylesterase 1	↑	0.04	12	15	7
P02760	protein AMBP	↑	0.05	11	20	7
P01042	kininogen-1	↑	0.02	10	44	8
P02766	transthyretin	↑	0.01	12	44	9
P02774	vitamin D-binding protein	↑	0.01	25	78	10
P01024	complement C3	↑	0.01	142	90	10

Table 2. continued

accession no.	protein name	FC (T2DM/Q)	p value	peptides CI (95%)	% coverage	MS/MS expt <sup>b</sup>
P0C0L5	complement C4-B	↑	0.02	55	75	10
P01023	$\alpha$ -2-macroglobulin	↑	0.02	137	62	10
P01008	antithrombin-III	↑	0.02	27	77	8
P02763	alpha-1-acid glycoprotein 1	↑	0.03	17	33	9
P01011	$\alpha$ -1-antichymotrypsin	↑	0.02	22	40	7
P05452	tetranectin	↑	0.02	9	19	8
O75882	attractin	↑	0.01	20	34	7
P00742	coagulation factor X	↑	0.03	3	31	8

<sup>a</sup>The FC represents fold change as a ratio of protein expression in T2DM patients as compared to nondiabetic controls. <sup>b</sup>Number of iTRAQ experiments in which the fold change (T2DM/C) significantly changed ( $p < 0.05$ ).

Table 3. Q1/Q3 transitions of 5 target proteins selected for the MRM experiments<sup>a</sup>

protein name	peptide sequence	parent ( $m/z$ ) (Q1)	transition ( $m/z$ ) (Q3)	dwelltime (s)	cone (V)	CE (V)	start position	end position
apolipoprotein-AI	ATEHLSTLSEK	406.07(+3)	522.32/363.13	0.184	25	15	220	230
	AKPALEDLR	338.45(+3)	506.85/288.19	0.157	25	15	231	239
vitamin D-binding protein	VPTADLEDVPLAEDITNI	789.80(+3)	1067.26/234.19	0.821	25	15	243	264
	ELPEHTVK	318.36(+3)	355.76/312.27	0.184	25	10	277	284
fibronectin	DLQFVEVTDVK	647.01 (+2)	936.27/690.20	0.157	25	15	912	922
	GATYNIIVEALK	646.66(+2)	672.25/637.32	0.157	25	15	2165	2176
afamin	IAPQLSTEELVSLGEK	572.01(+3)	765.33/533.16	0.157	25	10	438	453
	SDVGFLPPFTLDPEEK	944.58(+2)	619.21/502.13	0.157	25	15	131	147
transthyretin	GSPAINVAHVFR	456.47(+3)	558.16/322.78	0.157	25	15	42	54
	GPTGTGESK	417.21 (+2)	679.08/234.13	0.511	25	15	21	29
$\beta$ -galactosidase	GDFQFNISR	542.31 (+2)	636.33/262.23	0.157	25	20	954	962
	APLDNDIGVSEATR	729.36(+2)	718.96/175.08	0.157	25	25	787	801

<sup>a</sup>Two peptides per protein were selected for relative quantification of protein levels in 72 control and T2DM serum samples.  $\beta$ -Galactosidase peptides (residues 954-962, GDFQFNISR and residues 787-801 APLDNDIGVSEATR) were used as internal standards. Q1 represents the mass to charge ( $m/z$ ) ratio of the parent ion; and the Q3 represents the  $m/z$  ratio for the daughter ions for the respective Q1. The start and end positions indicate the sequence of the target protein. CE represents collision energy. V represents voltage used.

iTRAQ experiment performed with the larger cohort of 110 serum samples ( $n = 40$  controls and  $n = 70$  T2DM subjects). Five independent iTRAQ analyses were performed to gain statistical power. For subsequent validation of the iTRAQ data, MRM-MS was used for determination of relative levels of five target proteins, which showed significantly altered expression in the T2DM cohort.

#### Identification of Differentially Expressed Serum Proteins in T2DM Using iTRAQ-2D-LC-MS/MS

The depletion of high-abundance proteins from serum along with two-dimensional separation of serum proteins resulted in the identification of 227 high-confidence proteins corresponding to 1392 high confidence peptides, representing >40% sequence coverage for the identified protein and at least 3 high-confidence peptides (>95% CI). The molecular weight and  $pI$  distribution analysis of proteins was performed using ProteoIQ software (NuSep, USA), which revealed a broad range coverage of the serum proteome and an excellent overlap between the proteins detected in the control and T2DM samples, whereas a global comparison of the relative expression showed a significant change in the proteome of T2DM cohort (Figure 2, panels A and B, respectively). Gene ontology analysis indicated the participation of differentially expressed proteins in a diverse array of cellular functions, including metabolic and cellular processes, transport, cell cycle, and cell communication among others, emphasizing the systemic effects of T2DM (Figure 2, panel C). Some of the significantly altered proteins (fold change  $\geq 2$  with  $p$  values  $\leq 0.05$ ) are represented in Figure 2 (panel D); the rest are listed in Table 2. The significantly

changing complement factors are listed in Supporting Information Table ST2. Among these, apolipoprotein, a lipid transporter, has been previously shown to have a unique serum protein pattern, highlighting the association of the apolipoprotein family of proteins with family history with T2DM in a cohort-based study.<sup>33</sup>

iTRAQ analysis revealed the differential expression of selenoprotein P, which plays a critical role in selenium homeostasis and antioxidant response and has been reported to be dysregulated in T2DM.<sup>34,35,36,37</sup> High levels of circulating selenoprotein are associated with hypoadiponectinemia, inflammation, and atherosclerosis, commonly observed in T2DM patients.<sup>35,38</sup> Given the role of selenoprotein P in glucose regulation and insulin sensitivity associated with diabetes, this protein presents a promising potential target for therapy against T2DM.

Several metabolic dysfunctions in diabetes, such as glucose oxidation, nonenzymatic protein glycation, and ensuing degradation of these glycated proteins, produce large volumes of free radicals.<sup>39</sup> Thus, oxidative stress has been implicated to be inextricably linked to the pathophysiology of T2DM.<sup>40</sup> Interestingly, we noted significant changes in the serum levels of several oxidative stress biomarkers, such as  $\alpha$ -2HS-glycoprotein, hyaluronan-binding protein 2, and ceruloplasmin in T2DM patients when compared with healthy volunteers.<sup>41-44</sup>

In addition, patients diagnosed with T2MD are predisposed to higher risk of thromboembolism, in part due to abnormal homeostatic changes in blood coagulation mechanisms.<sup>45</sup> The



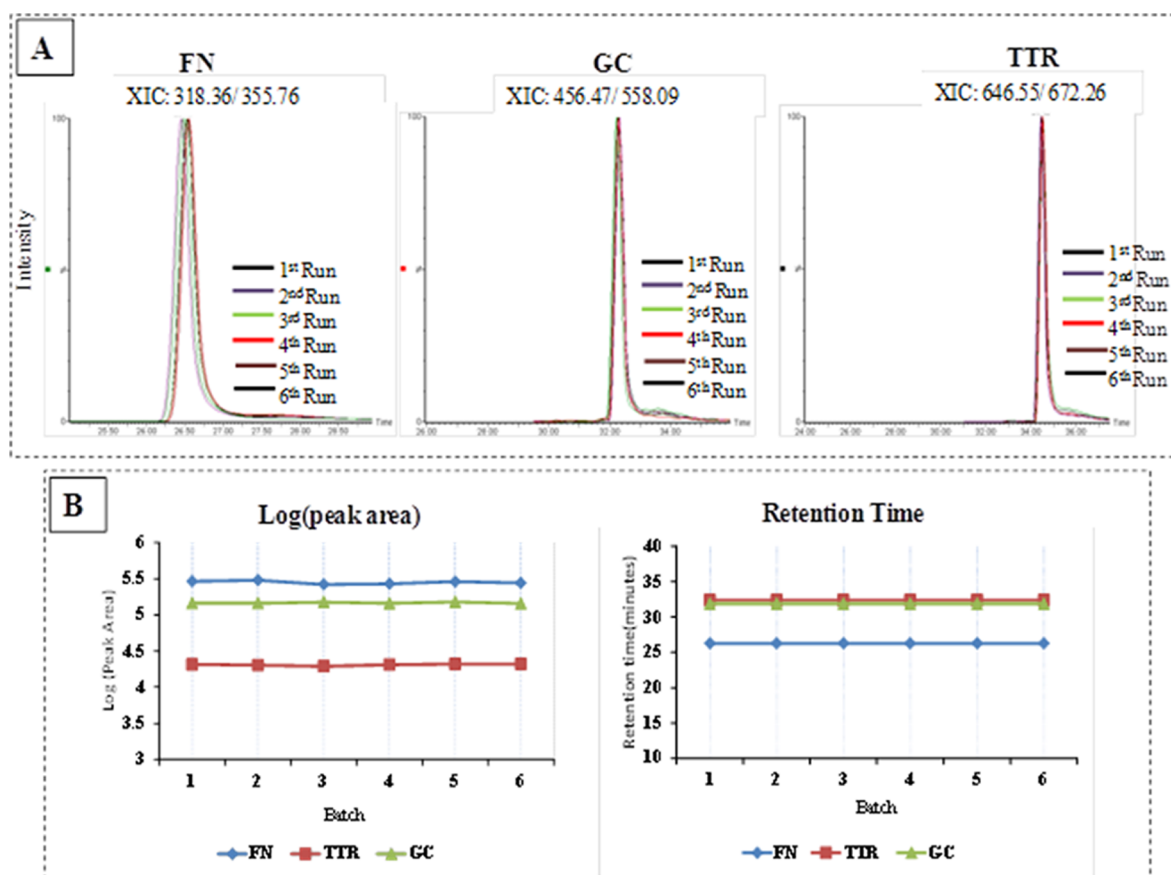


**Figure 3.** Reproducibility assessment of MRM runs. Six MRM runs were performed for fibronectin (FN), vitamin D-binding protein (GC), and transthyretin (TTR). Three serum samples (biological replicates) were independently processed, and the MRM data was acquired in duplicate (technical replicates). Extracted ion chromatogram (XIC), 318.36/355.76 for fibronectin; XIC, 456.47/558.09 vitamin D-binding protein; and XIC, 646.55/672.26 transthyretin were extracted to calculate the peak area and retention time. (Panel A) Chromatographic overlay of six injections for FN, GC, and TTR. (Panel B) The peak area and retention times remained consistent across the different acquisitions.

iTRAQ analysis showed an increase in the serum levels of fibronectin, plasminogen, prothrombin, and fibulin, which have been implicated in enhancing the thrombotic potential and angiopathic complications in T2DM patients.<sup>46</sup>

#### Targeted Quantitation of Five Proteins Using Multiple Reaction Monitoring (MRM-MS)

The discovery phase iTRAQ data augmented the identification of a number of putative biomarkers with implicated roles in the pathogenesis of T2DM and associated complications. Of these, apolipoprotein-A1, vitamin D-binding protein, fibronectin, afamin, and transthyretin were chosen for verification of differential abundance in T2DM patients, as compared with control subjects, using MRM-MS. These proteins were selected on the basis of their diverse and significant functions in mediating progression of T2DM per published reports.<sup>47,48,49–52</sup> Two high-confidence peptides with a rich product ion spectrum for each target protein were selected for relative quantification analysis using MRM. The transitions for each peptide are listed in Table 3. MRM was performed in individual samples in an independent cohort consisting of nondiabetic control subjects ( $n = 36$ ) and those diagnosed with T2DM ( $n = 36$ ).  $\beta$ -Galactosidase peptides were used as internal standards. For each peptide analyzed by MRM, the peak area was normalized to that of the internal standard peptide, and the standard deviation was calculated on the basis of the peptide transitions. For all peptides listed in Table 3, the most intense product ions,

mainly y ions, from the iTRAQ spectrum were amenable to MRM analysis.

The replication of MRM analysis depends on consistent sample preparation procedures and instrument performance. Hence, three biological replicates were analyzed in duplicate for three target proteins and assessed for retention time and chromatographic reproducibility (Figure 3) during MRM runs. The retention times as well as the XIC (extracted ion chromatogram) overlay for each target protein analyzed displayed sufficient reproducibility ( $SD < 0.01$ ) to facilitate measurements in undepleted serum samples. Furthermore, normalization to the peak area of the standard resulted in reduction of standard deviation in peak area calculations.

For each of the five target proteins selected, two transitions were monitored for each peptide (Supporting Information Figure S4A–J). One of the transitions was used for quantitation, and the second was used as a confirmatory ion. The MRM-MS data were exported into the TargetLynx, and the peak area of the transition was calculated by normalizing to the area of the  $\beta$ -galactosidase standard for each sample. This approach has been successfully used for the verification of biomarkers of diabetic nephropathy.<sup>16</sup>

The data was manually checked for accurate peak integration. The distribution of the normalized peak area transitions was interactively plotted, and the means were compared between the control subjects and the T2DM serum samples using the Wilcoxon Signed-rank test. ROC curves were also generated,

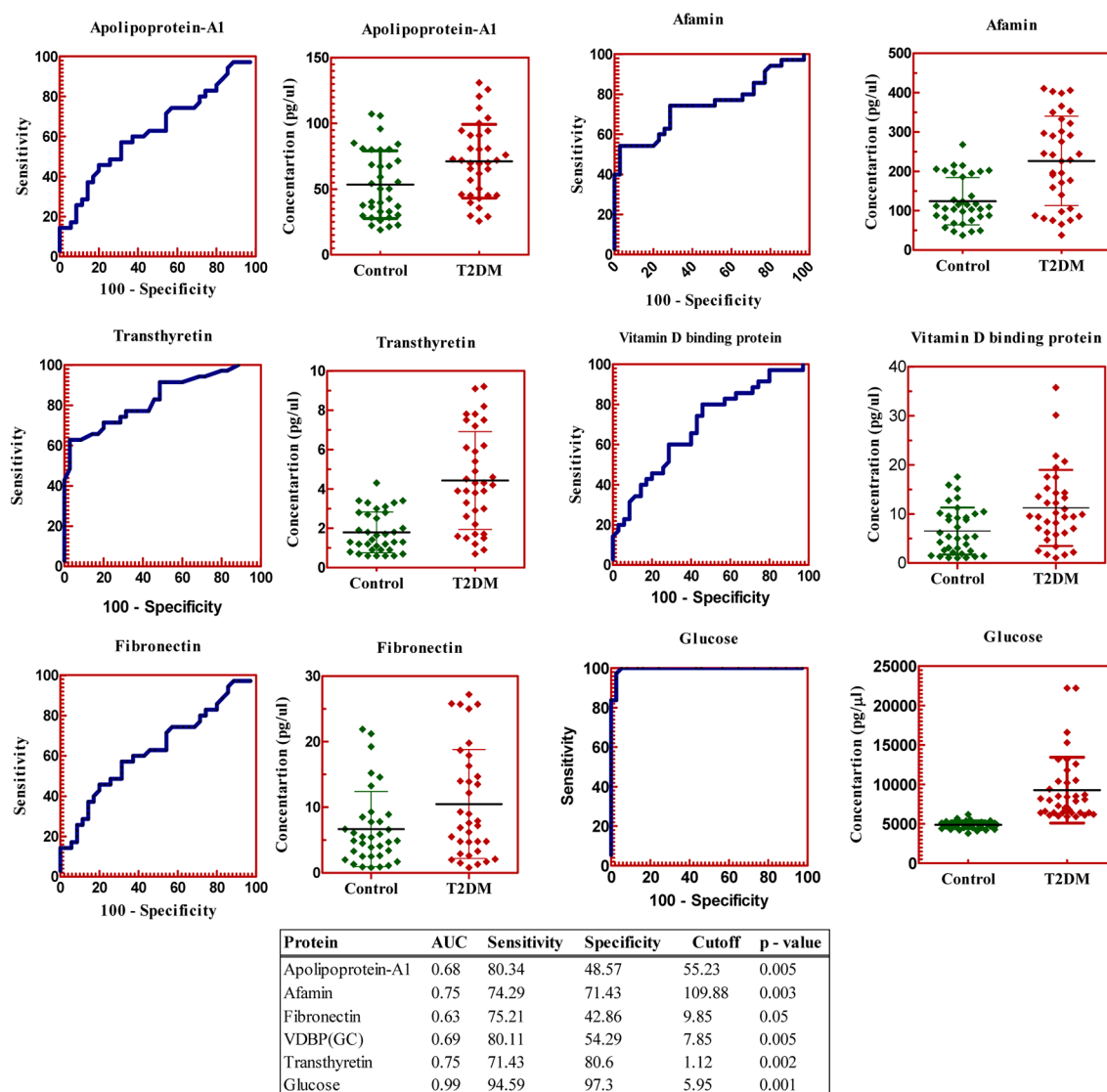


**Figure 4.** Targeted quantitation of serum peptides that showed significant differential expression in patients diagnosed with T2DM as compared to control subjects. The normalized area ratio (endogenous peptide/internal standard) for each peptide in individual control or T2DM serum samples were subjected to nonparametric analysis using the Wilcoxon test with a cut off  $p \leq 0.05$ . The solid lines in the ROC curves represent the plot of 1-specificity versus sensitivity, and the interactive plots of the distribution of the normalized concentration of the target protein in the two study groups. (VDBP: vitamin D-binding protein).

and the AUC (area under curve) was calculated (Figure 4). The MRM data were found to be very consistent with the iTRAQ data. Apolipoprotein-A1 (Apo-A1), vitamin D-binding protein (GC), fibronectin, afamin, and transthyretin were found to increase in the T2DM cohort. All tests were informative, with reasonably high sensitivity in all five markers with estimates of over 70%. Specificity, however, was high only in afamin and transthyretin. The AUC's, which quantify the overall ability to discriminate T2DM from controls, were all significantly greater than 0.5, indicating the usefulness of these markers for stratification and diagnosis. (Figure 4).

The respective cutoffs present the estimated thresholds for classifying patients as positive for T2DM. Screening for circulating diagnostic markers is beneficial for classifying patients who are predisposed to developing comorbidities that are known to be associated with T2DM. The results indicate that these markers can be potentially used not only for screening T2DM patients but also for risk stratification for various comorbidities such as diabetic nephropathy (trans-

thyretin and vitamin D-binding protein), cardiovascular disease (apolipoprotein-A1) and should be followed up with future studies aimed at dissecting the functionality of these proteins. The differential expression for six proteins (TTR, GC, Apo A1, ceruloplasmin, angiotensin, and gelsolin) determined by Western blots was in accordance with the iTRAQ and MRM data. In addition, two of these proteins, TTR and GC were further validated in the same cohort using Western blot and Q-PCR with  $p$  values less than 0.03 and 0.02, respectively (Supporting Information Figure S5). These results need to be validated in the future using a larger patient cohort. Interestingly, the specificity and sensitivity of glucose were 97.3 and 94.5, respectively, underscoring the gold standard efficacy of blood glucose levels as a discriminator between the normal and T2DM cohort.

#### Pathways Related to the Pathogenesis of T2DM

Functional pathway analysis was performed for the differentially expressed proteins in T2DM, identified via iTRAQ-based

Table 4. Functional Pathway Analysis of Biological Networks and Associated Diseases in T2DM Using the IPA Tool

top functions		Networks	score
		associated molecules	
lipid metabolism, small molecule biochemistry, neurological disease		A1BG, AHSG, AMBP, APOA1, APOA2, APOA4, APOB, APOC2, APOC3, APOD, APOH, APOL1, CP, GC, HABP2, HDL, HP, KLK3, KLKB1, NCOR-LXR-oxysterol-RXR-9 cisRA, NFkB, Nr1h, PKP1, PON1, SAA, SERPINA4, SERPINF2, SERPING1, Tcf 1/3/4, TF, TTR VLDL	58
cardiovascular disease, hematological disease, hematological system development and function		A2M, APOE, BCAM, CTRC, ERK1/2, FBLN1, fibrin, FN1, GSN, HRG, laminin, LRGI, LRP, LUM, Mlc, Pak, PARVA, PdGF, PDGF, BB, Pld, PLG, PROC, rock, SERPINA6, SERPIND1, Smad2/3, Tgf beta, THBS1	28
lipid metabolism, molecular transport, small molecule biochemistry		AFM, APOC2, APOE, APOL1, APP, BPIFA1, CAD, CARD16, CP, Cyp2c11l, ECE1, FXR ligand-FXR-retinoic acid-RXR $\alpha$ , GPR77, GPX3, Hba, HPR, IL6, IL1B, K3FC1, LXR ligand-LXR-retinoic acid-RXR $\alpha$ , PDHA1, SCARB1, SEPP1, SERPINA7, SERPINF2, SLC5A2, SPINT1, TMCC2, TPR, XPNPEP2	21
tissue morphology, cardiovascular system development and function, organ morphology		ADCY, AGT, Akt, ANK3, Apl, AZGP1, CD5L, cyclin A, DES, ERK, FSH, histone h3, IgG, IL1, KNG1, LDL, Mapk, Mek, Mmp, NADPH oxidase, P38 MAPK, PI3K, PIR, Pkc(s), Ras, TIMP4, Vegf	14

top functions		Diseases and Disorders	p value
		associated molecules	
cardiovascular disease		AGT, AHSG, APOA1, APOA4, APOB, APOC2, APOC3, APOE, APOH, FN1, GSN, HP, HRG, KNG1, PARVA, PLG, PON1, PROC, SERPIND1, THBS1	$2.83 \times 10^{-12}$ to $1.79 \times 10^{-03}$
neurological disease		A2M, AGT, APOA1, APOA2, APOA4, APOB, APOC2, APOC3, APOD, APOE, GC, HP, HRG, PLG, PON1, SEPP1, TF, TTR	$1.01 \times 10^{-11}$ to $2.62 \times 10^{-03}$
psychological disorder		A2M, AGT, APOA1, APOA2, APOA4, APOB, APOC2, APOC3, APOD, APOE, GC, HP, HRG, PLG, PON1, SEPP1, TF, TTR	$1.01 \times 10^{-11}$ to $7.98 \times 10^{-04}$
organismal injury and abnormalities		AGT, APOA1, APOA2, APOB, APOE, PLG, PON1, SERPIND1	$7.93 \times 10^{-11}$ to $2.99 \times 10^{-03}$
inflammatory response		AGT, APOE, APOH, FN1, GC, KLKB1, KNG1, PLG, SERPINF2, SERPING1, THBS1	$3.66 \times 10^{-09}$ to $3.37 \times 10^{-03}$

expression profiling. Lipid metabolism and small molecule biochemistry were identified as the top network perturbation (score = 58) (Table 4). Previously, gene polymorphism has been reported for the apolipoprotein family in T2DM, which can significantly alter circulating lipid levels.<sup>53</sup> We observed an increase in Apo A1 levels in the serum, which has been reported to cause atherogenic dyslipidemia.<sup>54</sup> CVD was the top disease in T2DM, which has been well documented. We also found the serum levels of transthyretin and angiotensin to be significantly altered in T2DM samples, which have been thought to contribute toward progression to CVD in T2DM patients.<sup>55–58</sup>

## DISCUSSION

The goal of this study was to use a discovery followed by verification pipeline to perform comparative serum proteomics analysis using a statistically significant clinical cohort for the identification of circulating biomarkers of T2DM. We report on the identification and verification of several biomarker candidates that can be potentially used for subset stratification of T2DM cohort. We identified a total of 227 high-confidence proteins corresponding to 1393 peptides with >95% confidence representing >40% sequence coverage. GO analysis predicted the differentially expressed proteins to be involved in a wide variety of cellular and metabolic processes. Many of these proteins showed a fold change of 2 or more between the control and T2DM serum samples. Five of these proteins—namely, apolipoprotein A1, afamin, transthyretin, fibronectin, and vitamin D-binding protein—were verified with MRM-based targeted proteomics in an independent cohort ( $n = 72$ ). In addition, TTR and GC were validated by Western blot as well as by Q-PCR.

We show that the combination of iTRAQ shotgun- and MRM-based targeted quantitative proteomics is a powerful tool for characterization of biomarkers in T2DM. In the initial discovery phase, serum samples from controls ( $n = 40$ ) and patients with T2DM ( $n = 70$ ) were randomly pooled within each group to generate five pools, which were then analyzed in

duplicate using five independent 4-plex iTRAQ experiments. In the verification phase, the target proteins were quantified in individual control ( $n = 36$ ) and T2DM samples ( $n = 36$ ) using UPLC–MRM–MS analysis.

Several published studies have reported proteomic alterations in diabetes. Thingholm et al. (2011) used a similar approach for a large scale proteomic study aimed at identifying and validating changes in protein abundance among human myotubes obtained from nondiabetic lean, nondiabetic obese, and type 2 diabetic subjects.<sup>59</sup> The clinical study reported here uses a similar approach; however, it is novel in terms of quantitative profiling and validation of circulating serum biomarkers in a direct comparative analysis of healthy and T2DM subjects. A limitation of this study was a difference in the mean age of the control and diabetic cohort. However, a subset analysis for the target proteins showed that these markers were differentially expressed in the diabetic cohort, regardless of the age of the individual (Supporting Information Table ST3).

A significant finding of our study was an increase in the serum levels of vitamin D-binding protein (GC) in T2DM patients. This was subsequently validated by MRM, Q-PCR, and Western blotting. Several studies suggest that 25-hydroxy vitamin D (GC-25OHD) is bound to GC, and this complex is freely filtered across the glomerulus and transported to the proximal tubule, where this complex is reabsorbed by megalin and gets converted into 1,25-dihydroxy vitamin D (the active form of vitamin D) by the hydroxylase activity of the proximal tubule epithelial cells.<sup>60</sup> Thrailkill (2009) reported the enhanced excretion of megalin in the urine of diabetic patients, which restricts the reabsorption of GC-25OHD, possibly leading to vitamin D deficiency.<sup>61</sup> Several cohort-based studies report the association of low levels of circulating vitamin D with modest to high risk of T2DM and associated comorbidities.<sup>62–65</sup> Thus, monitoring GC levels may help risk stratification of T2DM patients.

We also report the up-regulation of transthyretin and retinol-binding protein 4 (RBP4) in the T2DM cohort. Interaction network plots of TTR and RBP4, show that RBP4 binds with



TTR (Supporting Information Figure S6). This is interesting because elevated levels of TTR and RBP4 have been reported in patients presenting with obesity and metabolic syndrome.<sup>66–68</sup> The RBP4–TTR complex resists glomerular filtration, thereby reducing the clearance of RBP4. The levels of RBP4 seem to be regulated by kidney homeostasis rather than metabolic factors in patients with T2DM.<sup>69</sup> Taken together, these results suggest that managing the RBP4 levels in diabetic patients as a part of overall therapeutic strategy may have beneficial effects in this group.<sup>70,71</sup> As such, scoring for serum levels of RBP4 and TTR may be useful in screening for T2DM patients at high risk of developing diabetic nephropathy.

## CONCLUSIONS

In conclusion, iTRAQ-based two-dimensional LC–MS/MS serum profiling led to the identification of several differentially abundant proteins in T2DM, which represent diverse biological processes and cellular functions. The differential abundance was confirmed by MRM-MS, which is fast gaining ground as a sensitive, specific, and cost-effective methodology for relative quantification of protein biomarkers.

A significant percentage of T2DM patients are known to progress to nephropathy, cardiovascular disease, delayed wound healing capabilities, and diabetic retinopathy, indicating an inherent heterogeneity in T2DM patients.<sup>72–74</sup> However, the current treatment regimens for these patients are not customized so as to target individual pathology. Thus, a better understanding of biological pathways and molecular network perturbations and interactions is likely to advance our knowledge of the different subtypes of T2DM and facilitate the development of targeted therapeutics. Our study has revealed distinct molecular networks and metabolic pathways that were activated in T2DM. It is hoped that future studies with larger cohorts as well as those that focus on dissecting mechanistic roles will enhance our understanding of the pathogenesis of T2DM and contribute to the development of targeted therapeutics in accordance with the personalized medicine paradigm.<sup>75</sup>

## ASSOCIATED CONTENT

### Supporting Information

Additional information as noted in text. This material is available free of charge via the Internet at <http://pubs.acs.org>.

## AUTHOR INFORMATION

### Corresponding Author

\*Phone: (202)687-2756. Fax: (202)687-8860. E-mail: [akc27@georgetown.edu](mailto:akc27@georgetown.edu).

### Author Contributions

<sup>†</sup>These authors contributed equally to this work

### Notes

The authors declare no competing financial interest.

## ACKNOWLEDGMENTS

This publication was made possible by NPRP Grant No. 08-740-3-148 from the Qatar National Research Fund (a member of Qatar Foundation). The statements made herein are solely the responsibility of the authors. The authors acknowledge the Proteomics and Metabolomics shared resource and the Genomics and Epigenomics Shared Resource, supported in part by NIH/NCI Grant P30-CA051008, and the clinical

laboratory Hamad Medical Corporation (Doha, Qatar). The authors also thank Dr. Anju Preet for helping with the optimization of QPCR assay with serum samples and Dr. Troy Sulahian (Waters Corporation) for help with peptide MRM assays. The authors also thank Nusep, Inc. for providing the beta version of the ProteoIQ software for iTRAQ data analysis.

## REFERENCES

- (1) Gjesing, A. P.; Pedersen, O. 'Omics'-driven discoveries in prevention and treatment of type 2 diabetes. *Eur. J. Clin. Invest.* **2012**, *42* (6), 579–88.
- (2) Seshasai, S. R.; Kaptoge, S.; Thompson, A.; Di Angelantonio, E.; Gao, P.; Sarwar, N.; Whincup, P. H.; Mukamal, K. J.; Gillum, R. F.; Holme, I.; Njolstad, I.; Fletcher, A.; Nilsson, P.; Lewington, S.; Collins, R.; Gudnason, V.; Thompson, S. G.; Sattar, N.; Selvin, E.; Hu, F. B.; Danesh, J. Diabetes mellitus, fasting glucose, and risk of cause-specific death. *N. Engl. J. Med.* **2011**, *364* (9), 829–41.
- (3) Kolberg, J. A.; Jorgensen, T.; Gerwien, R. W.; Hamren, S.; McKenna, M. P.; Moler, E.; Rowe, M. W.; Urdea, M. S.; Xu, X. M.; Hansen, T.; Pedersen, O.; Borch-Johnsen, K. Development of a type 2 diabetes risk model from a panel of serum biomarkers from the Inter99 cohort. *Diabetes Care* **2009**, *32* (7), 1207–12.
- (4) Tuomilehto, J.; Lindstrom, J.; Eriksson, J. G.; Valle, T. T.; Hamalainen, H.; Ilanne-Parikka, P.; Keinanen-Kiukkaanniemi, S.; Laakso, M.; Louheranta, A.; Rastas, M.; Salminen, V.; Uusitupa, M. Prevention of type 2 diabetes mellitus by changes in lifestyle among subjects with impaired glucose tolerance. *N. Engl. J. Med.* **2001**, *344* (18), 1343–50.
- (5) Abdul-Ghani, M. A.; Williams, K.; DeFronzo, R. A.; Stern, M. What is the best predictor of future type 2 diabetes? *Diabetes Care* **2007**, *30* (6), 1544–8.
- (6) Wilson, P. W.; Meigs, J. B.; Sullivan, L.; Fox, C. S.; Nathan, D. M.; D'Agostino, R. B., Sr. Prediction of incident diabetes mellitus in middle-aged adults: the Framingham Offspring Study. *Arch. Intern. Med.* **2007**, *167* (10), 1068–74.
- (7) Lapolla, A.; Porcu, S.; Traldi, P. Some views on proteomics in diabetes. *Clin. Chem. Lab. Med.* **2011**, *49* (6), 943–57.
- (8) Sundsten, T.; Ortsater, H. Proteomics in diabetes research. *Mol. Cell. Endocrinol.* **2009**, *297* (1–2), 93–103.
- (9) Herder, C.; Karakas, M.; Koenig, W. Biomarkers for the prediction of type 2 diabetes and cardiovascular disease. *Clin. Pharmacol. Ther.* **2011**, *90* (1), 52–66.
- (10) Nakatani, S.; Kakehashi, A.; Ishimura, E.; Yamano, S.; Mori, K.; Wei, M.; Inaba, M.; Wanibuchi, H. Targeted proteomics of isolated glomeruli from the kidneys of diabetic rats: sorbin and SH3 domain containing 2 is a novel protein associated with diabetic nephropathy. *Exp. Diabetes Res.* **2011**, *2011*, 979354.
- (11) Mullen, W.; Delles, C.; Mischak, H. Urinary proteomics in the assessment of chronic kidney disease. *Curr. Opin. Nephrol. Hypertens.* **2011**, *20* (6), 654–61.
- (12) Prunotto, M.; Ghiggeri, G.; Bruschi, M.; Gabbiani, G.; Lescuyer, P.; Hoher, B.; Chaykovska, L.; Berrera, M.; Moll, S. Renal fibrosis and proteomics: current knowledge and still key open questions for proteomic investigation. *J. Proteomics* **2011**, *74* (10), 1855–70.
- (13) Kim, H. J.; Kim, P. K.; Yoo, H. S.; Kim, C. W. Comparison of tear proteins between healthy and early diabetic retinopathy patients. *Clin. Biochem.* **2012**, *45* (1–2), 60–7.
- (14) Merchant, M. L.; Klein, J. B. Proteomic discovery of diabetic nephropathy biomarkers. *Adv. Chronic Kidney Dis.* **2010**, *17* (6), 480–6.
- (15) VanGuilder, H. D.; Bixler, G. V.; Kutzler, L.; Brucklacher, R. M.; Bronson, S. K.; Kimball, S. R.; Freeman, W. M. Multi-modal proteomic analysis of retinal protein expression alterations in a rat model of diabetic retinopathy. *PLoS One* **2011**, *6* (1), e16271.
- (16) Kim, K.; Kim, S. J.; Yu, H. G.; Yu, J.; Park, K. S.; Jang, I. J.; Kim, Y. Verification of biomarkers for diabetic retinopathy by multiple reaction monitoring. *J. Proteome Res.* **2010**, *9* (2), 689–99.



- (17) Collins, H. W.; Buettger, C.; Matschinsky, F. High-resolution two-dimensional polyacrylamide gel electrophoresis reveals a glucose-response protein of 65 kDa in pancreatic islet cells. *Proc. Natl. Acad. Sci. U.S.A.* **1990**, *87* (14), 5494–8.
- (18) Collins, H.; Najafi, H.; Buettger, C.; Rombeau, J.; Settle, R. G.; Matschinsky, F. M. Identification of glucose response proteins in two biological models of beta-cell adaptation to chronic high glucose exposure. *J. Biol. Chem.* **1992**, *267* (2), 1357–66.
- (19) Fernandez, C.; Fransson, U.; Hallgard, E.; Spegel, P.; Holm, C.; Krogh, M.; Warell, K.; James, P.; Mulder, H. Metabolomic and proteomic analysis of a clonal insulin-producing beta-cell line (INS-1 832/13). *J. Proteome Res.* **2008**, *7* (1), 400–11.
- (20) Zhang, R.; Barker, L.; Pinchev, D.; Marshall, J.; Rasamoeliso, M.; Smith, C.; Kupchak, P.; Kireeva, I.; Ingratta, L.; Jackowski, G. Mining biomarkers in human sera using proteomic tools. *Proteomics* **2004**, *4* (1), 244–56.
- (21) Tsuneki, H.; Ishizuka, M.; Terasawa, M.; Wu, J.-B.; Sasaoka, T.; Kimura, O. Effect of green tea on blood glucose levels and serum proteomic patterns in diabetic (db/db) mice and on glucose metabolism in healthy humans. *BMC Pharmacol.* **2004**, *4*, 8.
- (22) Kiga, C.; Nakagawa, T.; Koizumi, K.; Sakurai, H.; Shibagaki, Y.; Ogawa, K.; Goto, H.; Saiki, I. Expression patterns of plasma proteins in spontaneously diabetic rats after oral administration of a Kampo medicine, Hachimi-jio-gan, using SELDI ProteinChip platform. *Biol. Pharm. Bull.* **2005**, *28* (6), 1031–7.
- (23) Jiang, M.; Jia, L.; Jiang, W.; Hu, X.; Zhou, H.; Gao, X.; Lu, Z.; Zhang, Z. Protein dysregulation in red blood cell membranes of type 2 diabetic patients. *Biochem. Biophys. Res. Commun.* **2003**, *309* (1), 196–200.
- (24) Friedewald, W. T.; Levy, R. I.; Fredrickson, D. S. Estimation of the concentration of low-density lipoprotein cholesterol in plasma, without use of the preparative ultracentrifuge. *Clin. Chem.* **1972**, *18* (6), 499–502.
- (25) Cham, B. E.; Knowles, B. R. A solvent system for delipidation of plasma or serum without protein precipitation. *J. Lipid Res.* **1976**, *17* (2), 176–81.
- (26) Tirumalai, R. S.; Chan, K. C.; Prieto, D. A.; Issaq, H. J.; Conrads, T. P.; Veenstra, T. D. Characterization of the low molecular weight human serum proteome. *Mol. Cell. Proteomics* **2003**, *2* (10), 1096–103.
- (27) Bradford, M. M. A rapid and sensitive method for the quantitation of microgram quantities of protein utilizing the principle of protein-dye binding. *Anal. Biochem.* **1976**, *72*, 248–54.
- (28) Karp, N. A.; Lilley, K. S. Investigating sample pooling strategies for DIGE experiments to address biological variability. *Proteomics* **2009**, *9* (2), 388–97.
- (29) Weinkauf, M.; Hiddemann, W.; Dreyling, M. Sample pooling in 2-D gel electrophoresis: a new approach to reduce nonspecific expression background. *Electrophoresis* **2006**, *27* (22), 4555–8.
- (30) Apweiler, R.; Bairoch, A.; Wu, C. H.; Barker, W. C.; Boeckmann, B.; Ferro, S.; Gasteiger, E.; Huang, H.; Lopez, R.; Magrane, M.; Martin, M. J.; Natale, D. A.; O'Donovan, C.; Redaschi, N.; Yeh, L. S. UniProt: the Universal Protein knowledgebase. *Nucleic Acids Res.* **2004**, *32* (Database issue), D115–9.
- (31) Weyer, C.; Hanson, R. L.; Tataranni, P. A.; Bogardus, C.; Pratley, R. E. A high fasting plasma insulin concentration predicts type 2 diabetes independent of insulin resistance: evidence for a pathogenic role of relative hyperinsulinemia. *Diabetes* **2000**, *49* (12), 2094–101.
- (32) Escoffier, P.; Paris, L.; Bodaghi, B.; Danis, M.; Mazier, D.; Marinach-Patrice, C. Pooling aqueous humor samples: bias in 2D-LC-MS/MS strategy? *J. Proteome Res.* **2010**, *9* (2), 789–97.
- (33) Sundsten, T.; Ostenson, C. G.; Bergsten, P. Serum protein patterns in newly diagnosed type 2 diabetes mellitus—influence of diabetic environment and family history of diabetes. *Diabetes Metab. Res. Rev.* **2008**, *24* (2), 148–54.
- (34) Burk, R. F.; Hill, K. E.; Selenoprotein, P. An extracellular protein with unique physical characteristics and a role in selenium homeostasis. *Annu. Rev. Nutr.* **2005**, *25*, 215–35.
- (35) Misu, H.; Ishikura, K.; Kurita, S.; Takeshita, Y.; Ota, T.; Saito, Y.; Takahashi, K.; Kaneko, S.; Takamura, T. Inverse correlation between serum levels of selenoprotein P and adiponectin in patients with type 2 diabetes. *PLoS One* **2012**, *7* (4), e34952.
- (36) Speckmann, B.; Sies, H.; Steinbrenner, H. Attenuation of hepatic expression and secretion of selenoprotein P by metformin. *Biochem. Biophys. Res. Commun.* **2009**, *387* (1), 158–63.
- (37) Roman, M.; Lapolla, A.; Jitaru, P.; Sechi, A.; Cosma, C.; Cozzi, G.; Cescon, P.; Barbante, C. Plasma selenoproteins concentrations in type 2 diabetes mellitus—a pilot study. *Transl. Res* **2010**, *156* (4), 242–50.
- (38) Yang, S. J.; Hwang, S. Y.; Choi, H. Y.; Yoo, H. J.; Seo, J. A.; Kim, S. G.; Kim, N. H.; Baik, S. H.; Choi, D. S.; Choi, K. M. Serum selenoprotein P levels in patients with type 2 diabetes and prediabetes: implications for insulin resistance, inflammation, and atherosclerosis. *J. Clin. Endocrinol. Metab.* **2011**, *96* (8), E1325–9.
- (39) Maritim, A. C.; Sanders, R. A.; Watkins, J. B., 3rd. Diabetes, oxidative stress, and antioxidants: a review. *J. Biochem. Mol. Toxicol.* **2003**, *17* (1), 24–38.
- (40) Drews, G.; Krippeit-Drews, P.; Dufer, M. Oxidative stress and beta-cell dysfunction. *Pflugers Arch.* **2010**, *460* (4), 703–18.
- (41) Lehtinen, A. B.; Burdon, K. P.; Lewis, J. P.; Langefeld, C. D.; Ziegler, J. T.; Rich, S. S.; Register, T. C.; Carr, J. J.; Freedman, B. I.; Bowden, D. W. Association of alpha-2-Heremans-Schmid glycoprotein polymorphisms with subclinical atherosclerosis. *J. Clin. Endocrinol. Metab.* **2007**, *92* (1), 345–52.
- (42) Kodama, K.; Horikoshi, M.; Toda, K.; Yamada, S.; Hara, K.; Irie, J.; Sirota, M.; Morgan, A. A.; Chen, R.; Ohtsu, H.; Maeda, S.; Kadowaki, T.; Butte, A. J. Expression-based genome-wide association study links the receptor CD44 in adipose tissue with type 2 diabetes. *Proc. Natl. Acad. Sci. U.S.A.* **2012**, *109* (18), 7049–54.
- (43) Bajorath, J.; Greenfield, B.; Munro, S. B.; Day, A. J.; Aruffo, A. Identification of CD44 residues important for hyaluronan binding and delineation of the binding site. *J. Biol. Chem.* **1998**, *273* (1), 338–43.
- (44) Savu, O.; Ionescu-Tirgoviste, C.; Atanasiu, V.; Gaman, L.; Papacoea, R.; Stoian, I. Increase in total antioxidant capacity of plasma despite high levels of oxidative stress in uncomplicated type 2 diabetes mellitus. *J. Int. Med. Res.* **2012**, *40* (2), 709–16.
- (45) Kwaan, H. C. Changes in blood coagulation, platelet function, and plasminogen-plasmin system in diabetes. *Diabetes* **1992**, *41* (Suppl 2), 32–5.
- (46) Piazza, G.; Goldhaber, S. Z.; Kroll, A.; Goldberg, R. J.; Emery, C.; Spencer, F. A. Venous thromboembolism in patients with diabetes mellitus. *Am. J. Med.* **2012**, *125* (7), 709–16.
- (47) Liu, W.; Lan, T.; Xie, X.; Huang, K.; Peng, J.; Huang, J.; Shen, X.; Liu, P.; Huang, H. S1P2 receptor mediates sphingosine-1-phosphate-induced fibronectin expression via MAPK signaling pathway in mesangial cells under high glucose condition. *Exp. Cell Res.* **2012**, *318* (8), 936–43.
- (48) Takiishi, T.; Gysemans, C.; Bouillon, R.; Mathieu, C. Vitamin D and diabetes. *Endocrinol. Metab. Clin. North Am.* **2010**, *39* (2), 419–46 table of contents.
- (49) Ando, Y. Transthyretin: its miracle function and pathogenesis. *Rinsho Byori* **2009**, *57* (3), 228–35.
- (50) Buxbaum, J. N.; Reixach, N. Transthyretin: the servant of many masters. *Cell. Mol. Life Sci.* **2009**, *66* (19), 3095–101.
- (51) Hermo, R.; Mier, C.; Mazzotta, M.; Tsuji, M.; Kimura, S.; Gugliucci, A. Circulating levels of nitrated apolipoprotein A-I are increased in type 2 diabetic patients. *Clin. Chem. Lab. Med.* **2005**, *43* (6), 601–6.
- (52) Speckaert, M.; Huang, G.; Delanghe, J. R.; Taes, Y. E. Biological and clinical aspects of the vitamin D binding protein (Gc-globulin) and its polymorphism. *Clin. Chim. Acta* **2006**, *372* (1–2), 33–42.
- (53) Chaudhary, R.; Likidilid, A.; Peerapatdit, T.; Tresukosol, D.; Srisuma, S.; Ratanamaneechat, S.; Sriratanasathavorn, C. Apolipoprotein E gene polymorphism: effects on plasma lipids and risk of type 2 diabetes and coronary artery disease. *Cardiovasc. Diabetol.* **2012**, *11*, 36.

- (54) Chapman, M. J. Pitavastatin: novel effects on lipid parameters. *Atheroscler. Suppl.* **2011**, *12* (3), 277–84.
- (55) Cangemi, C.; Skov, V.; Poulsen, M. K.; Funder, J.; Twal, W. O.; Gall, M. A.; Hjortdal, V.; Jespersen, M. L.; Kruse, T. A.; Aagard, J.; Parving, H. H.; Knudsen, S.; Hoilund-Carlsen, P. F.; Rossing, P.; Henriksen, J. E.; Argraves, W. S.; Rasmussen, L. M. Fibulin-1 is a marker for arterial extracellular matrix alterations in type 2 diabetes. *Clin. Chem.* **2011**, *57* (11), 1556–65.
- (56) Garcia-Pavia, P.; Avellana, P.; Bornstein, B.; Heine-Suner, D.; Cobo-Marcos, M.; Gomez-Bueno, M.; Segovia, J.; Alonso-Pulpon, L. A. Familial approach in hereditary transthyretin cardiac amyloidosis. *Rev. Esp. Cardiol.* **2011**, *64* (6), 523–6.
- (57) Gouni-Berthold, I.; Krone, W.; Berthold, H. K. Vitamin D and cardiovascular disease. *Curr. Vasc. Pharmacol.* **2009**, *7* (3), 414–22.
- (58) Li, R.; Nicklas, B.; Pahor, M.; Newman, A.; Sutton-Tyrrell, K.; Harris, T.; Lakatta, E.; Bauer, D. C.; Ding, J.; Satterfield, S.; Kritchevsky, S. B. Polymorphisms of angiotensinogen and angiotensin-converting enzyme associated with lower extremity arterial disease in the Health, Aging and Body Composition study. *J. Human Hypertens.* **2007**, *21* (8), 673–82.
- (59) Thingholm, T. E.; Bak, S.; Beck-Nielsen, H.; Jensen, O. N.; Gaster, M. Characterization of human myotubes from type 2 diabetic and nondiabetic subjects using complementary quantitative mass spectrometric methods. *Mol. Cell. Proteomics* **2011**, *10* (9), M110 006650.
- (60) Negri, A. L. Proximal tubule endocytic apparatus as the specific renal uptake mechanism for vitamin D-binding protein/25-(OH)D3 complex. *Nephrology (Carlton)* **2006**, *11* (6), 510–5.
- (61) Thrallkill, K. M.; Nimmo, T.; Bunn, R. C.; Cockrell, G. E.; Moreau, C. S.; Mackintosh, S.; Edmondson, R. D.; Fowlkes, J. L. Microalbuminuria in type 1 diabetes is associated with enhanced excretion of the endocytic multiligand receptors megalin and cubilin. *Diabetes Care* **2009**, *32* (7), 1266–8.
- (62) Marckmann, P.; Agerskov, H.; Thinesh Kumar, S.; Bladbjerg, E. M.; Sidelmann, J. J.; Jespersen, J.; Nybo, M.; Rasmussen, L. M.; Hansen, D.; Scholze, A. Randomized controlled trial of cholecalciferol supplementation in chronic kidney disease patients with hypovitaminosis D. *Nephrol. Dial. Transplant.* **2012**, *27* (9), 3523–31.
- (63) Chailurkit, L. O.; Aekplakorn, W.; Ongphiphadhanakul, B. The association between vitamin D status and type 2 diabetes in a Thai population, a cross-sectional study. *Clin. Endocrinol (Oxford)* **2012**, *77* (5), 658–64.
- (64) Forouhi, N. G.; Ye, Z.; Rickard, A. P.; Khaw, K. T.; Luben, R.; Langenberg, C.; Wareham, N. J. Circulating 25-hydroxyvitamin D concentration and the risk of type 2 diabetes: results from the European Prospective Investigation into Cancer (EPIC)-Norfolk cohort and updated meta-analysis of prospective studies. *Diabetologia* **2012**, *55* (8), 2173–82.
- (65) Makariou, S.; Liberopoulos, E.; Florentin, M.; Lagos, K.; Gazi, I.; Challa, A.; Elisaf, M. The relationship of vitamin D with non-traditional risk factors for cardiovascular disease in subjects with metabolic syndrome. *Arch. Med. Sci.* **2012**, *8* (3), 437–43.
- (66) Kloting, N.; Graham, T. E.; Berndt, J.; Kralisch, S.; Kovacs, P.; Wason, C. J.; Fasshauer, M.; Schon, M. R.; Stumvoll, M.; Bluher, M.; Kahn, B. B. Serum retinol-binding protein is more highly expressed in visceral than in subcutaneous adipose tissue and is a marker of intra-abdominal fat mass. *Cell. Metab.* **2007**, *6* (1), 79–87.
- (67) Fernandez-Real, J. M.; Moreno, J. M.; Ricart, W. Circulating retinol-binding protein-4 concentration might reflect insulin resistance-associated iron overload. *Diabetes* **2008**, *57* (7), 1918–25.
- (68) Raila, J.; Henze, A.; Spranger, J.; Mohlig, M.; Pfeiffer, A. F.; Schweigert, F. J. Microalbuminuria is a major determinant of elevated plasma retinol-binding protein 4 in type 2 diabetic patients. *Kidney Int.* **2007**, *72* (4), 505–11.
- (69) Akbay, E.; Muslu, N.; Nayir, E.; Ozhan, O.; Kiykim, A. Serum retinol binding protein 4 level is related with renal functions in Type 2 diabetes. *J. Endocrinol. Invest.* **2010**, *33* (10), 725–9.
- (70) Motani, A.; Wang, Z.; Conn, M.; Siegler, K.; Zhang, Y.; Liu, Q.; Johnstone, S.; Xu, H.; Thibault, S.; Wang, Y.; Fan, P.; Connors, R.; Le, H.; Xu, G.; Walker, N.; Shan, B.; Coward, P. Identification and characterization of a non-retinoid ligand for retinol-binding protein 4 which lowers serum retinol-binding protein 4 levels in vivo. *J. Biol. Chem.* **2009**, *284* (12), 7673–80.
- (71) Mody, N.; Graham, T. E.; Tsuji, Y.; Yang, Q.; Kahn, B. B. Decreased clearance of serum retinol-binding protein and elevated levels of transthyretin in insulin-resistant ob/ob mice. *Am. J. Physiol. Endocrinol. Metab.* **2008**, *294* (4), E785–93.
- (72) Khan, S. R. Is oxidative stress, a link between nephrolithiasis and obesity, hypertension, diabetes, chronic kidney disease, metabolic syndrome? *Urol. Res.* **2012**, *40* (2), 95–112.
- (73) Athyros, V. G.; Elisaf, M. S.; Alexandrides, T.; Achimastos, A.; Ganotakis, E.; Biliannou, E.; Karagiannis, A.; Liberopoulos, E. N.; Tziomalos, K.; Mikhailidis, D. P. Long-term impact of multifactorial treatment on new-onset diabetes and related cardiovascular events in metabolic syndrome: a post hoc ATTEMPT analysis. *Angiology* **2012**, *63* (5), 358–66.
- (74) Tian, J.; Wen, Y.; Yan, L.; Cheng, H.; Yang, H.; Wang, J.; Kozman, H.; Villarreal, D.; Liu, K. Vascular endothelial dysfunction in patients with newly diagnosed type 2 diabetes and effects of 2-year and 5-year multifactorial intervention. *Echocardiography* **2011**, *28* (10), 1133–40.
- (75) Hood, L.; Flores, M. A personal view on systems medicine and the emergence of proactive P4 medicine: predictive, preventive, personalized and participatory. *N. Biotechnol.* **2012**, *29* (6), 613–24.